Adaptive Duty Cycling in Sensor Networks via Continuous Time Markov Chain Modelling

Ronald Chan*, Pengfei Zhang†, Wenyu Zhang‡, Ido Nevat*,
Alvin Valera*, Hwee-Xian Tan* and Natarajan Gautam§
*Institute for Infocomm Research (I^{2}R), Singapore
†School of Electrical Engineering, Nanyang Technological University (NTU), Singapore
‡Department of Statistics, Cornell University, New York, United States
§Industrial and Systems Engineering, Texas A&M University, Texas, United States

***Abstract*—The dynamic and unpredictable nature of energy harvesting sources that are used in wireless sensor networks necessitates the need for adaptive duty cycling techniques. Such adaptive control allows sensor nodes to achieve energy-neutrality, whereby both energy supply and demand are balanced.**

This paper proposes a framework enabling an adaptive duty cycling scheme for sensor networks that takes into account the operating duty cycle of the node, and application-level QoS requirements. We model the system as a Continuous Time Markov Chain (CTMC), and derive analytical expressions for key QoS metrics - such as latency, loss probability and power consumption. We then formulate and solve the optimal operating duty cycle as a non-linear optimization problem, using latency and loss probability as the constraints. Simulation results show that a Markovian duty cycling scheme can outperform periodic duty cycling schemes.

I. Introduction

Wireless sensor networks can be used in a large number of applications, such as environmental and structural health monitoring, weather forecasting [1]–[3], surveillance, health care, and home automation [3], [4]. A key challenge that constrains the operation of sensor networks is limited lifetime arising from the finite energy storage in each node. Recent advances in energy harvesting techniques [5] can potentially eliminate the limited lifetime problem in sensor networks and enable perpetual operation without the need for battery replacement, which is not only laborious and expensive, but also infeasible in certain situations.

Despite this, the continuous or uninterrupted operation of energy harvesting-powered sensor networks remains a major challenge, due to the unpredictable and dynamic nature of the harvested energy supply [6], [7]. To cope with the energy supply dynamics, adaptive duty cycling techniques [6], [8], [9] have been proposed. The common underlying objective of these techniques is to attain an optimal *energy-neutral* point at every node, wherein the energy supply and energy demand are balanced. Unfortunately, state-of-the-art adaptive duty cycling techniques focus primarily on obtaining the optimal per-node duty cycle to prolong network lifetime, while neglecting application-level quality of service (QoS) requirements.

In this paper, we propose a framework enabling an adaptive duty cycling scheme that allows network designers to trade-off between QoS requirements and the operating duty cycle. Figure 1 illustrates the main components of such a scheme, which comprises the: (i) energy harvesting controller; (ii) adaptive duty cycle controller; and (iii) wakeup scheduler.

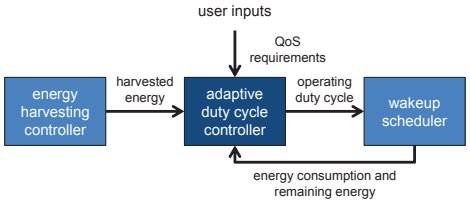

Fig. 1. Main components of proposed adaptive duty cycling scheme.

The adaptive duty cycle controller computes the optimal operating duty cycle based on user inputs (in the form of application QoS requirements) and the available amount of harvested energy. The wakeup scheduler will then: (i) manage the sleep and wake interfaces of each node, based on the recommended operating duty cycle, and (ii) provide feedback to the adaptive duty cycle controller on the energy consumption of and remaining energy in the node. This feedback loop allows the duty cycle controller to **adapt** its duty cycle, based on the harvested energy and the remaining energy - in order to meet QoS requirements - based on operating policies such as energy neutrality.

The focus of the work in this paper is on the duty cycle controller, which is key to the energy-aware operations of a sensor network. Using a Continuous Time Markov Chain (CTMC) model, we derive key QoS metrics including *loss probability*, *latency*, as well as *power consumption*, as functions of the duty cycle. We then formulate and solve the optimal operating duty cycle as a non-linear optimization problem, using latency and loss probability as the constraints. We validate our CTMC model through Monte Carlo simulations, and show through simulations that a Markovian duty cycling scheme can outperform periodic duty cycling schemes.

The rest of the paper is organized as follows. Section II provides details on the key assumptions used in our system model. In Section III, we derive network performance metrics using the CTMC model. Simulation results are presented in Section IV. Section V concludes the paper.

II. System Model

In this section, we highlight the key assumptions in our work and provide details of various system components, such as the traffic model, channel model and transmission schemes.

1) Node State: Each node v_j is in one of the following states $N_j \in \{0, 1\}$ at any point in time, where $N_j = 0$ and $N_j = 1$ denote that v_j is in the *asleep* and *awake* states respectively. The duration t that node v_j is in each of the states N_j is a random variable that follows an exponential distribution, given by:

$$p(t) = \begin{cases} \gamma_i \cdot e^{-\gamma_i \cdot t} & t \geq 0 \\ 0 & t < 0, \end{cases} \quad (1)$$

where γ_i, $i \in \{0, 1\}$ are the respective rates of the asleep state $N_j = 0$ and awake state $N_j = 1$. We define the average cycle time as $T = \frac{1}{\gamma_0} + \frac{1}{\gamma_1}$. Then, the average long-term fraction of time that the node is in the *awake* state is given by $q = \frac{1}{\gamma_1 \cdot T}$.

2) Traffic Model: The number of data packets d_0 that are generated by each node follows a Poisson distribution with an average rate of λ_0 packets per unit time, i.e., $d_0 \sim \text{Pois}(\lambda_0)$. In addition, the node receives d_n packets from all of its neighbours according to a Poisson process at an average rate of λ packets per unit time, i.e., $d_n \sim \text{Pois}(\lambda)$.

3) Channel Model: The time-varying wireless link quality is modelled by the classical Gilbert-Elliot Markovian model [10], [11] with two states $L \in \{0, 1\}$ - where $L = 0$ and $L = 1$ denote that the channel quality is *bad* and *good* respectively. The duration t that a node is in each of the channel states is a random variable that follows an exponential distribution, given by:

$$p(t) = \begin{cases} c_i \cdot e^{-c_i \cdot t} & t \geq 0 \\ 0 & t < 0, \end{cases} \quad (2)$$

where c_i, $i \in \{0, 1\}$ are the respective rates of the *bad* and *good* states. We let β and α denote the probabilities of successfully delivered data packets when the channel is in the *bad* and *good* states respectively. Acknowledgement packets are assumed to always be delivered successfully.

4) Probing Mechanism: The network utilizes probes to determine if an arbitrary downstream node v_k is in the awake state $N_k = 1$, prior to the commencement of data transmission. The probing mechanism is modelled as a Poisson process, with intensities θ_g and θ_b when the channel quality is in the good and poor states respectively. The reception of a probe-acknowledgement by the transmitter node v_j indicates that the downstream node v_k is awake; transmitter node v_j will then instantaneously transmit *all* its data packets to node v_k.

5) Transmission Schemes: We consider two transmission schemes: X_n (without retransmissions) and X_r (with retransmissions). Under transmission scheme X_n, data packets that have not been successfully delivered to the receiver (due to poor channel quality) will **not** be retransmitted. The corresponding average number of packets that successfully arrive at a node under good and poor channel conditions are denoted as λ_g and λ_b respectively, where $\lambda_b = \frac{\beta \cdot \lambda_g}{\alpha}$. Under transmission scheme X_r, data packets are retransmitted until they are successfully delivered to the receiver. The corresponding average number of packets that successfully arrive under this scheme is λ, where $\lambda_g = \lambda_b = \lambda$. The effective packet arrival rate when the node is in the awake state is $\frac{\lambda}{q}$.

6) Power Consumption: The power consumptions of a node in the asleep and awake states are P_{asleep} and P_{awake} respectively. The power consumption of the probing mechanisms is denoted as P_{probe}. The energy incurred to transmit a single data packet is $\mathcal{E}_{tx}$.

III. Continuous Time Markov Chain Model

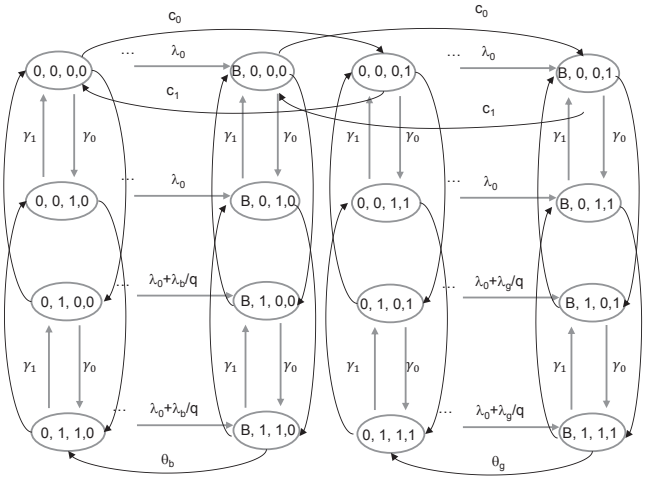

Fig. 2. Continuous Time Markov Chain model of the network with transition matrix $\mathcal{Q}$.

With the definitions provided in the previous section, we can now build a suitable probabilistic model to describe the performance of the wireless sensor network. To this end, we model the system as a CTMC (as shown in Figure 2).

A. CTMC State Space

We consider a 4-tuple CTMC state space as follows:

1) Node buffer: Each node has a FIFO buffer of finite size B. The number of packets in the finite queue is denoted by $b \in \{0, 1, \ldots, B\}$.
2) Node state: As mentioned in Section II, each node v_j is in state $N_j \in \{0, 1\}$ at any one time, depending on whether it is *asleep* ($N_j = 0$) or *awake* ($N_j = 1$).
3) Downstream node state: An arbitrary downstream (receiving) node v_k is in state $N_k \in \{0, 1\}$ at any one time, depending on whether it is *asleep* ($N_k = 0$) or *awake* ($N_k = 1$).
4) Link quality: The wireless link quality is in state $L \in \{0, 1\}$ at any one time, depending on whether the channel is *bad* ($L = 0$) or *good* ($L = 1$).

Given these definitions, the state space $\mathcal{S}$ can be written as the following Cartesian product: $\mathcal{S} = \{0, 1, \ldots, B\} \times \{0, 1\} \times \{0, 1\} \times \{0, 1\} \in \mathcal{R}^{|b| \times |N_j| \times |N_k| \times |L|}$. The corresponding cardinality of the state space is given by $|\mathcal{S}| = 8(B + 1)$.

B. Modeling QoS metrics

We model the following key QoS metrics in wireless networks: (i) *average power consumption* incurred by a node; (ii) *latency* incurred by holding packets in the transmission queue; and (iii) *loss probability* due to wireless channel transmission errors and packet drops arising from buffer overflows.

To calculate these QoS metrics, we first solve the steady state probabilities of the CTMC system, i.e. the long term probabilities of being in each state of the state space. The steady-state probability of an arbitrary state $s_k \in \mathcal{S}$ is given by $p_k = \lim_{t\to\infty} P_r(\mathcal{S}(t) = s_k)$. We let $\mathrm{p} = [p_1\ p_2\ ...\ p_{|\mathcal{S}|}]$. The steady state probabilities can then be obtained by solving $\mathrm{p}\mathcal{Q} = \mathbf{0}$ and $\sum_{s_k\in\mathcal{S}} p_k = 1$, where $\mathcal{Q}$ is the transition matrix of the CTMC.

We now define the QoS metrics, as follows:

1) *Loss probability* $\pi(q)$: The loss probability $\pi(q)$ describes the event that there is incoming traffic (either from the node itself or its neighbors), when the buffer is already full, for a given duty cycle q. This is given by:

$$\begin{aligned}\pi(q) =& P_r(b = B|d_0 = 0, d_n = 1)+\\ & P_r(b = B|d_0 = 1, d_n = 0).\end{aligned} \tag{3}$$

2) *Latency* $\ell(q)$: The latency ℓ is given by Little's Law $\ell = \frac{\bar{b}}{\lambda_e}$, where $\bar{b}$ is the average number of packets in the buffer, and λ_e is the effective packet arrival rate at the node.

$$\ell(q) = \mathbb{E}[\frac{b}{\lambda + \lambda_0}]. \tag{4}$$

3) *Average power consumption* $\rho(q)$: The average power consumption ρ of a node v_j is the sum of the power expended for the probing mechanism, packet transmissions, and other normal operations in each node state.

$$\begin{aligned}\rho(q) =& \mathcal{P}_{asleep}P_r(N_j = 0)+\\ & (\mathcal{P}_{awake} + \mathcal{P}_{probe})P_r(N_j = 1)+\\ & (\lambda + \lambda_0)\mathcal{E}_{tx}.\end{aligned} \tag{5}$$

We derive these quantities in (6) to (11) for the two transmission schemes X_r (with transmissions) and X_n (without retransmissions) as described in Section II.

C. Optimal Duty Cycle

Our objective is to find the optimal duty cycle q to minimize the power consumption, while satisfying application-level QoS constraints. This can be expressed as:

$$\begin{aligned} q =& \arg\min_q \rho(q)\\ \text{s.t.}\quad \pi(q) \leq& \pi_0\\ \ell(q) \leq& \ell_0\\ q \geq& 0\end{aligned} \tag{12}$$

where π_0 and ℓ_0 are pre-defined latency and loss thresholds.

Recall that γ_1 and γ_0 can be expressed as functions of q and the average cycle time T, as follows:

$$\begin{aligned}\gamma_1 &= \frac{1}{T\cdot q}\\ \gamma_0 &= \frac{1}{T\cdot(1-q)}\end{aligned} \tag{13}$$

Thus, we can further simplify the optimisation problem to a single parameter optimization problem by defining T and solving for γ_1 and γ_0.

Although the optimization problem in (12) does not have an analytical closed form expression, it is a single parameter optimisation problem. As such, it is easy to find the optimal q (denoted as q^*) numerically via simple evaluation on a finely divided grid.

IV. Simulation Results

In this section, we verify our theoretical model with Monte Carlo simulations, compare the effects of having Markovian and periodic duty cycles, and investigate the impact of our model parameters on the performance of the system. Table I summarizes the system parameters that are used in this section.

A. Model Verification

We verify the model as described in Sections II and III, through the use of Monte Carlo simulations in MATLAB to demonstrate the convergence of the results from randomly selected system instances towards the theoretical predictions in the model.

We study the performance of the QoS metrics between the theoretical model and Monte Carlo simulations, under two transmission schemes: (i) X_n - without retransmissions; and (ii) X_r - with retransmissions. Figure 3 shows that there is a good fit between the model and the Monte Carlo simulations, across the metrics - latency ℓ, loss probability π and average power consumption ρ. This highlights the validity of our proposed model in estimating the network performance.

B. Comparing Markovian and Periodic Systems

Conventionally, systems are duty-cycled via a periodic sleep-wake cycle. In order to generalize our results to more types of systems, we compare our results from the theoretical model (with Markovian sleep and wake times) with Monte Carlo simulations that have periodic sleep-wake cycles, taking care to ensure that the phase shift between the sleep-wake cycle of the node in question and the sleep-wake cycle of the recipient node is uniformly distributed across all possible values in the periodic case. In Figure 4, we plot the variation of the QoS parameters of latency, loss probability and average power consumption with respect to the duty cycle, once again for two sets of system parameters and for the models with and without retransmission.

In general, we expect that the Markovian system will perform as well as, if not better than, the periodic system, since the fixed nature of the sleep-wake scheduling in the periodic system may prevent it from receiving some of the exponentially arriving packets by virtue of the invariant periodicity. We observe that this appears to be the case for the loss probability. On the other hand, the Markovian

Transmission Scheme X_r (with retransmissions):

$$\pi(q) = \sum_{k=0}^{1} \frac{p_{B,1,0,k}(\lambda/q+\lambda_0)}{\lambda/q+\lambda_0+\gamma_0+\gamma_1+c_k} + \sum_{k=0}^{1} \frac{p_{B,1,1,k}(\lambda/q+\lambda_0)}{\lambda/q+\lambda_0+2\gamma_1+\theta+c_k} + \sum_{k=0}^{1} \frac{p_{B,0,0,k}\lambda_0}{\lambda_0+2\gamma_0+c_k} + \sum_{k=0}^{1} \frac{p_{B,0,1,k}\lambda_0}{\lambda_0+\gamma_0+\gamma_1+c_k} \quad (6)$$

$$\ell(q) = \frac{1}{\lambda+\lambda_0} \sum_{b=0}^{B}\sum_{i=0}^{1}\sum_{j=0}^{1}\sum_{k=0}^{1} bp_{b,i,j,k} \quad (7)$$

$$\rho(q) = \mathcal{P}_{asleep} \sum_{b=0}^{B}\sum_{j=0}^{1}\sum_{k=0}^{1} p_{b,0,j,k} + \mathcal{P}_{awake} \sum_{b=0}^{B}\sum_{j=0}^{1}\sum_{k=0}^{1} p_{b,1,j,k} + \mathcal{P}_{probe} \sum_{b=1}^{B}\sum_{j=0}^{1}\sum_{k=0}^{1} p_{b,1,j,k} + (\frac{\lambda}{1-\beta/\alpha}+\lambda_0)\mathcal{E}_{tx} \quad (8)$$

Transmission Scheme X_n (no retransmission):

$$\pi(q) = \frac{p_{B,1,0,0}(\lambda_b/q+\lambda_0)}{\lambda_b/q+\lambda_0+\gamma_0+\gamma_1+c_0} + \frac{p_{B,1,1,0}(\lambda_b/q+\lambda_0)}{\lambda_b/q+\lambda_0+2\gamma_1+\theta+c_0} + \frac{p_{B,0,0,0}\lambda_0}{\lambda_0+2\gamma_0+c_0} + \frac{p_{B,0,1,0}\lambda_0}{\lambda_0+\gamma_0+\gamma_1+c_0} + \frac{p_{B,1,0,1}(\lambda_g/q+\lambda_0)}{\lambda_g/q+\lambda_0+\gamma_0+\gamma_1+c_1} + \frac{p_{B,1,1,1}(\lambda_g/q+\lambda_0)}{\lambda_g/q+\lambda_0+2\gamma_0+\gamma_1+c_1} + \frac{p_{B,0,0,1}\lambda_0}{\lambda_0+2\gamma_0+c_1} + \frac{p_{B,0,1,1}\lambda_0}{\lambda_0+\gamma_0+\gamma_1+c_1} \quad (9)$$

$$\ell(q) = \frac{1}{\lambda_b+\lambda_0} \sum_{b=0}^{B}\sum_{i=0}^{1}\sum_{j=0}^{1} bp_{b,i,j,0} + \frac{1}{\lambda_g+\lambda_0} \sum_{b=0}^{B}\sum_{i=0}^{1}\sum_{j=0}^{1} bp_{b,i,j,1} \quad (10)$$

$$\rho(q) = \mathcal{P}_{asleep} \sum_{b=0}^{B}\sum_{j=0}^{1}\sum_{k=0}^{1} p_{b,0,j,k} + \mathcal{P}_{awake} \sum_{b=0}^{B}\sum_{j=0}^{1}\sum_{k=0}^{1} p_{b,1,j,k} + \mathcal{P}_{probe} \sum_{b=1}^{B}\sum_{j=0}^{1}\sum_{k=0}^{1} p_{b,1,j,k} + (\lambda+\lambda_0)\mathcal{E}_{tx} \quad (11)$$

TABLE I

SYSTEM PARAMETERS USED FOR THE VARIOUS FIGURES IN THIS DOCUMENT. V DENOTES A VARYING PARAMETER. FOR ALL FIGURES, $\beta/\alpha = 0.6$, $\lambda_0 = 0.01$, $\mathcal{P}_{\text{ASLEEP}} = \mathcal{E}_{\text{TX}} = 0.001$, $\mathcal{P}_{\text{AWAKE}} = 1$, AND $\mathcal{P}_{\text{PROBE}} = \mathcal{E}_{\text{TX}}\theta$. FOR ALL MONTE CARLO SIMULATIONS, 50 TRIALS WERE PERFORMED FOR EACH VALUE OF q.

Figure	3 (A)	3 (B)	4 (A)	4 (B)	5	6	7	8	9(a)	9(b)	9(c)
B	10	10	10	50	V	10	10	10	10	10	10
θ (X_r) or θ_g (X_n)	10	10	1	10	10	V	10	10	10	3	10
λ (X_r) or λ_g (X_n)	1	10	10	10	10	10	V	10	10	3	10
c_0	0.5	0.1	0.5	0.5	0.5	0.5	0.5	1	0.5	0.5	0.1
c_1	0.5	0.9	0.5	0.5	0.5	0.5	0.5	V	0.5	0.5	2

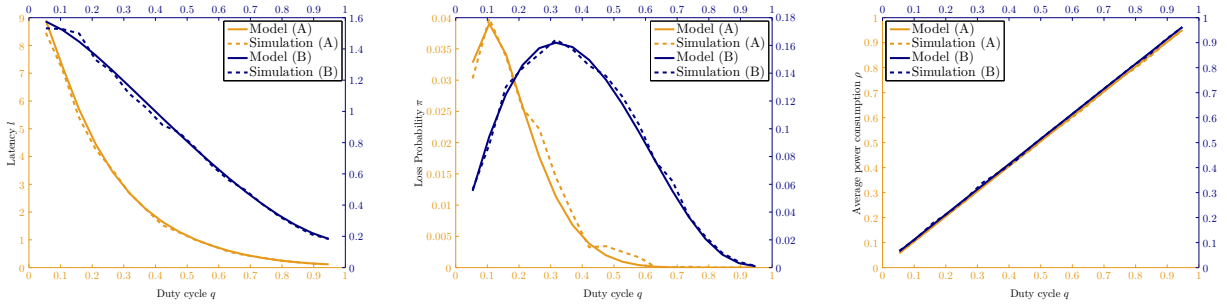

(a) Latency ℓ (b) Loss probability π (c) Average power consumption ρ

Fig. 3. Comparison between theoretical model and Monte Carlo simulations. Parameter set (A) uses transmission scheme X_r, while (B) uses X_n.

system provides good estimates for the latency and the average power consumption in the periodic system, as these two QoS parameters have a more direct dependence on the duty cycle.

C. Performance under Varying Model Parameters

1) Buffer Size B: Figure 5 studies the network performance under varying buffer sizes B. As buffer size increases, more packets can accumulate and fewer packets are dropped, resulting in higher latencies and lower loss probabilities.

2) Probing Rate θ: Figure 6 studies the network performance with varying probing rates θ. With higher probing rates, the data buffer is cleared more quickly, resulting in a decrease in both the latency and loss probability.

3) Packet Arrival Rate λ: Figure 7 illustrates the network performance for varying arrival rates λ. The effects of λ dominate those of θ at small rates: decreasing θ below λ does not influence the performance significantly. Also, faster arrival rates generate faster turnover and lower latencies, but

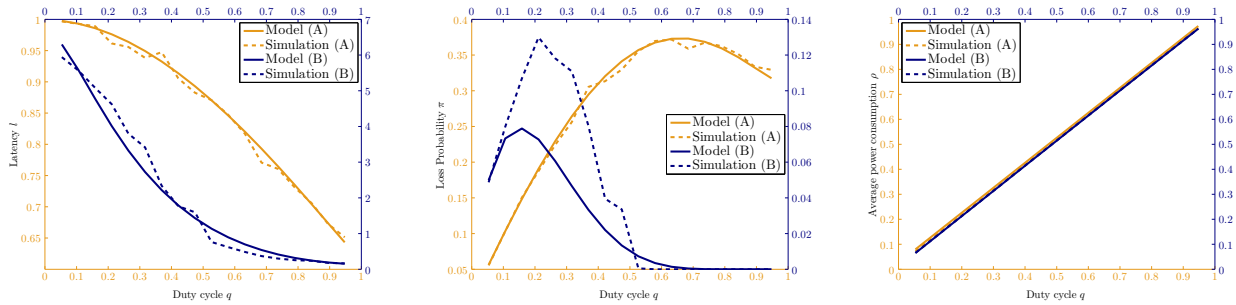

(a) Latency ℓ (b) Loss probability π (c) Average power consumption ρ

Fig. 4. Comparison between theoretical model with Markovian sleep-wake times and Monte Carlo simulations with periodic sleep-wake times. Parameter set (A) uses transmission scheme X_r, while (B) uses X_n.

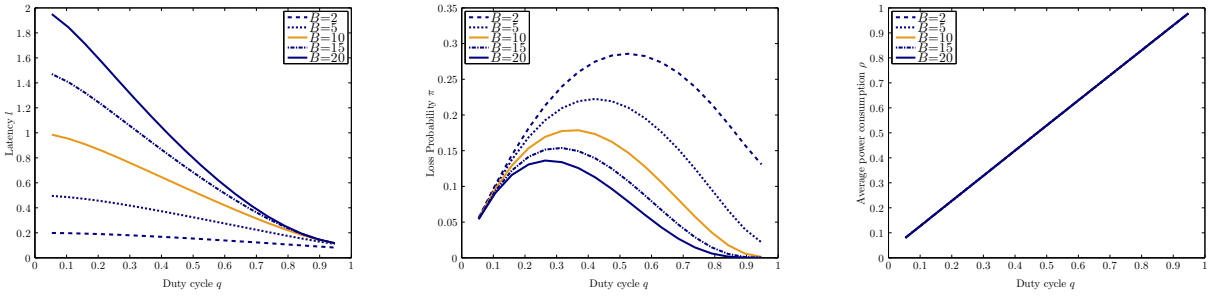

(a) Latency ℓ (b) Loss probability π (c) Average power consumption ρ

Fig. 5. Performance of QoS parameters for theoretical model with varying buffer size B, under transmission scheme X_r (with retransmissions).

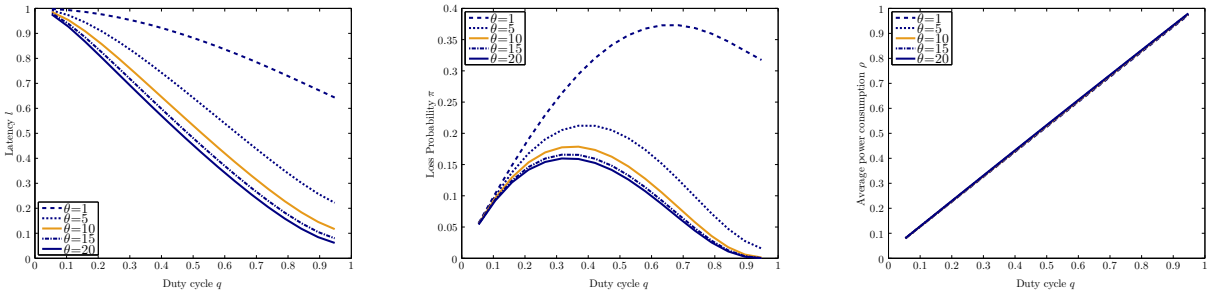

(a) Latency ℓ (b) Loss probability π (c) Average power consumption ρ

Fig. 6. Performance of QoS parameters for theoretical model with varying probing rate θ, under transmission scheme X_r (with retransmissions).

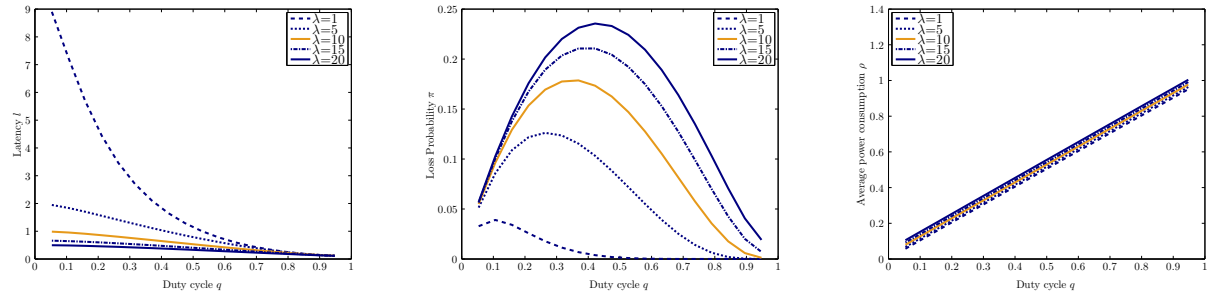

(a) Latency ℓ (b) Loss probability π (c) Average power consumption ρ

Fig. 7. Performance of QoS parameters for theoretical model with varying packet arrival rate λ, under transmission scheme X_r (with retransmissions).

more dropped packets and larger loss probabilities.

4) Link Quality and Retransmissions: Figure 8 studies the performance of the network for varying link quality

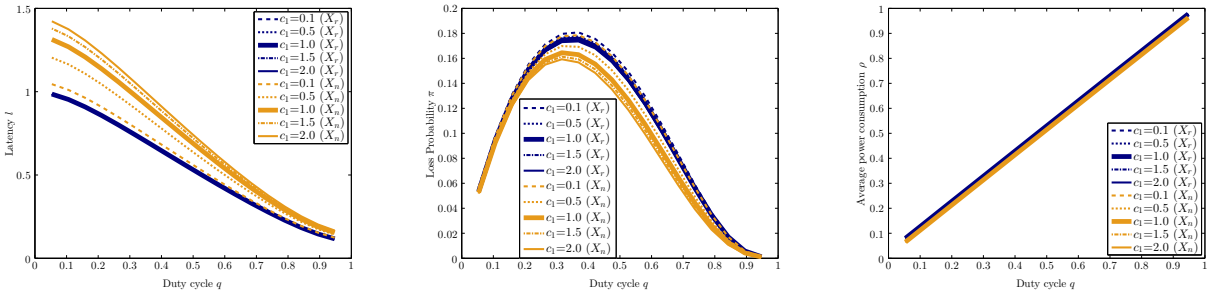

(a) Latency ℓ (b) Loss probability π (c) Average power consumption ρ

Fig. 8. Performance of QoS parameters for theoretical model with varying good-to-bad link quality transition rate c_1, under transmission schemes X_r and X_n.

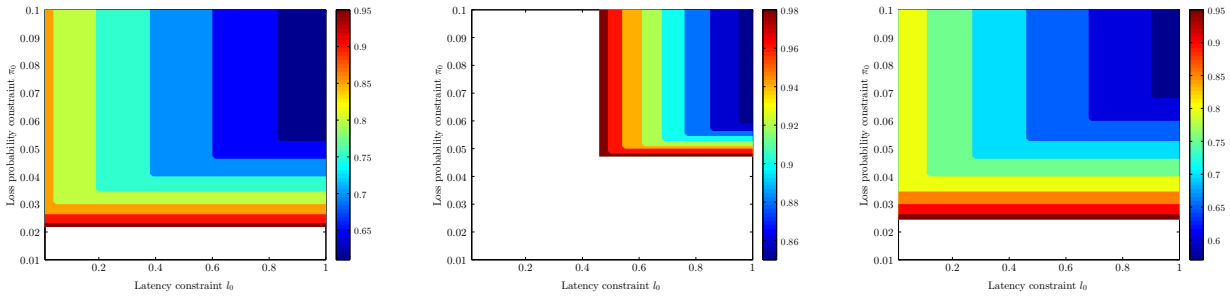

(a) (b) (c)

Fig. 9. Optimal duty cycle as a function of the QoS constraints for different sets of system parameters. In this plot, the optimal duty cycle is represented by a colour whose corresponding value can be read off from the colour bar. Steps are observed in the plot because the duty cycle was sampled discretely.

transition rates, under the different transmission schemes X_n and X_r. The system with X_r maintains its packet arrival and transmission rate even when the link quality is poor. Thus, it has a lower latency than the system with X_n, as suggested by (4). In the case of the latter, a higher transition rate for good-to-bad link quality further increases the latency.

D. Optimal Duty Cycle

Figure 9 plots the optimal duty cycle of the system after constraint optimization, for various latency and loss probability constraints, as well as different sets of system parameters. As expected, the optimum duty cycle required increases with lower latency and loss probability requirements. In addition, note that there exists regions in which the given constraints cannot be satisfied with the given input system parameters.

V. Conclusion

In this paper, we propose an adaptive duty cycling scheme in wireless sensor networks that takes into account application-level QoS requirements. A Continuous Time Markov Chain (CTMC) model is used to derive analytical expressions for these QoS metrics - such as latency, loss probability and average energy consumption - while considering practical system factors such as link quality variations and limited buffer sizes. Simulations show that the Markovian scheme highlighted in this work can outperform conventional periodic duty cycling schemes.

References

[1] A. Kottas, Z. Wang, and A. Rodrguez, "Spatial modeling for risk assessment of extreme values from environmental time series: a bayesian nonparametric approach," *Environmetrics*, vol. 23, no. 8, 2012.

[2] C. Fonseca and H. Ferreira, "Stability and contagion measures for spatial extreme value analyses," *arXiv preprint arXiv:1206.1228*, 2012.

[3] J. P. French and S. R. Sain, "Spatio-temporal exceedance locations and confidence regions," *Annals of Applied Statistics. Prepress*, 2013.

[4] I. Akyildiz, W. Su, Y. Sankarasubramaniam, and E. Cayirci, "Wireless sensor networks: a survey," *Computer networks*, vol. 38, no. 4, pp. 393–422, 2002.

[5] S. Sudevalayam and P. Kulkarni, "Energy harvesting sensor nodes: Survey and implications," *IEEE Communications Surveys Tutorials*, no. 99, pp. 1–19, 2010.

[6] A. Kansal, J. Hsu, S. Zahedi, and M. B. Srivastava, "Power management in energy harvesting sensor networks," *ACM Trans. Emb. Comput. Sys.*, vol. 6, pp. 1–38, Sep. 2007.

[7] Y. Gu, T. Zhu, and T. He, "Esc: Energy synchronized communication in sustainable sensor networks," in *Proc. IEEE ICNP*, 2009.

[8] C. Vigorito, D. Ganesan, and A. Barto, "Adaptive control of duty cycling in energy-harvesting wireless sensor networks," in *Proc. IEEE SECON*, 2007.

[9] T. Zhu, Z. Zhong, Y. Gu, T. He, and Z.-L. Zhang, "Leakage-aware energy synchronization for wireless sensor networks," in *Proc. ACM MobiSys*, 2009.

[10] E. N. Gilbert, "Capacity of a burst-noise channel," *Bell System Technical Journal*, vol. 39, no. 5, 1960.

[11] E. O. Elliot, "Estimates of error rates for codes on burst-noise channels," *Bell System Technical Journal*, vol. 42, no. 5, 1963.